RESEARCH ARTICLE

Predefined Time Nonsingular Fast Terminal Sliding Mode Control for Trajectory Tracking of ROVs

GUOYAN YU, ZHUOCHENG LI[ID], HAITAO LIU[ID], (Member, IEEE), AND QIHENG ZHU
School of Mechanical Engineering, Guangdong Ocean University, Zhanjiang 524088, China
Guangdong Provincial Marine Equipment and Manufacturing Engineering Technology Research Center, Zhanjiang 524088, China

Corresponding author: Zhuocheng Li (1204146125@qq.com)

ABSTRACT A predetermined time nonsingular fast terminal sliding mode control (PTNFTSMC) is proposed to solve the problem of long convergence time and instability in the orbit control of remotely operated vehicles (ROVs). First, a new concise method is proposed to design a predetermined-time controller by setting control parameter conditions that self-adjust according to the system state. Then, the control law of PTNFTSMC is formulated by combining the proposed theory of prescribed time control and the theory of fast termination nonsingular sliding control mode. Finally, the stability and tunability of the proposed controller in a specific period are demonstrated by rigorous arguments. Simulation experiments show that the proposed PTNFTSMC achieves stability at any initial state of the system for a specified time with guaranteed convergence accuracy, and the actual convergence time of the system is very close to the parameters of the specified time compared with other existing control schemes. This confirms the effectiveness and superiority of the proposed PTNFTSMC.

I. INTRODUCTION

The ocean, especially the deep sea, is rich in mineral and biological resources and is an expansion of human living space. The rational exploration, development, and utilization of marine resources will greatly promote a human society in the direction of sustainable development [1]. A remotely operated vehicle (ROV) is an unmanned underwater robot that transmits control signals and collects information through a series of cables connected to a master console. Compared to autonomous underwater vehicles (AUVs), ROVs are the best choice for specific investigations that tend to be conducted underwater because they can transmit information in real time and can freely switch between automatic operation and

The associate editor coordinating the review of this manuscript and approving it for publication was Shihong Ding[ID].

manual control modes [2]. However, the uncertainty of the ROV model and unpredictable external disturbance design of a suitable controller to ensure stable motion and fast dynamic response of the ROV is a great challenge [3]. On the one hand, the mathematical model of the ROV is highly nonlinear and strongly coupled, and its hydrodynamic parameters, estimated by software or obtained from tank experiments, differ from actual values. On the other hand, in the oceanic operating environment, ROVs are subject to unpredictable external disturbances such as waves and currents. With these complex factors, the control performance of the traditional linear control of the ROV is significantly reduced and cannot provide high-precision motion control capability [4].

For these reasons, several different control technologies have been applied to the control of ROVs in recent years, such as PID control [5], [6], backstepping control [7], [8],

sliding mode control (SMC) [9], [10], [11], [12], fuzzy logic control (FLC) [13], [14], [15], group optimization algorithm control [16], [17] and adaptive control [18], [19], [20]. However, all of the above control methods use asymptotic Lyapunov stability analysis to solve the trajectory tracking problem of ROVs, and theoretically, the trajectory tracking error takes infinite time to converge to the equilibrium state. However, in practice, a fast and stable response is one of the most important and desirable features of ROV trajectory tracking. Therefore, in practice, it is necessary to develop control systems that can achieve ROV convergence in a finite time.

With the increasing development of finite-time control technology [21], [22], [23], several finite-time controllers have been designed and applied to the field of underwater robot control. In [24], an AUV trajectory tracking controller was designed based on finite-time control theory and a consensus tracking control algorithm, combined with a finite-time observer to estimate its state information. In [25], an AUV trajectory tracking controller was designed based on finite-time control theory and supertwisting sliding mode control theory. In [26], finite-time control theory and sliding mode control theory with fast integration constraints, as well as a multi-AUV orbit tracking controller combined with neural networks, were developed. All of the above control methods are effective in converging the system error to zero in finite time. However, the finite-time convergence of the above schemes is highly dependent on the initial state of the system, and the effective convergence time increases when the initial state of the system is far from the equilibrium point, so the above schemes may not provide fast convergence when the initial state of the system increases significantly.

The above fixed time effectively solves the problem that the convergence time of the system depends on the initial state of the system, but the estimation of its convergence time needs to be calculated using multiple control parameters in the controller and cannot be adjusted directly by the designer, and changing the control parameters will have a significant impact on the convergence performance of the controller, which is not conducive to the reasonable allocation of the system convergence time. To solve this problem, an advanced stability control concept, i.e., a predefined time control strategy, has been recently proposed [27], [28], [29], [30]. The convergence time estimate of this control strategy is a predefined time parameter, which can be adjusted to maintain the actual convergence time of the system within the designer's preset time and achieve the tunability of system convergence. Recently, [31], [32] applied predefined time control to complex second-order systems such as rigid spacecraft and underwater robots and realized that the system convergence time can be adjusted by the time parameter. However, the aforementioned control strategies [27], [28], [29], [30], [31], [32] suffer from a complex and tedious design process and conservative convergence time estimation, i.e., the actual convergence time of the system
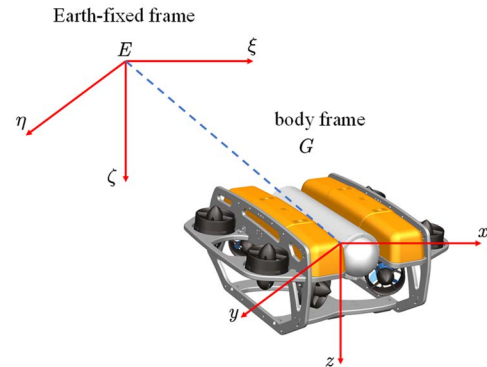

FIGURE 1. Coordinate systems of the ROV.

is smaller than the predefined convergence time. Based on this, a predefined nonsingular fast terminal sliding mode control is proposed in this paper for the trajectory tracking problem of ROVs. The main contributions of this paper are as follows.

(1) A new predefined time controller design method is proposed to ensure system convergence time tunability while simplifying the design process of existing predefined time controllers.

(2) By combining the new predefined time control scheme with the nonsingular fast terminal sliding mode control scheme, the controller can adjust the dominant convergence term by itself according to the system state, which makes the actual convergence time of the system very close to the predefined convergence time and greatly improves the adjustment accuracy of the system convergence time.

(3) The stability and convergence time tunability of the proposed predefined-time nonlinear fast terminal sliding mode controller is critically demonstrated, and the feasibility and superiority of the control scheme are verified using comparative simulation experiments.

The rest of this paper is as follows. Section II introduces the mathematical model of an ROV and the underlying theories of finite-time convergence, fixed-time convergence, and predefined-time convergence. Section III describes the design process of predefined nonsingular fast terminal sliding mode control and provides rigorous proof of controller stability and convergence time tunability. Section IV presents the proposed control scheme with three existing control schemes for comparative simulation experiments. Section V concludes the paper.

II. PRELIMINARIES AND PROBLEM DESCRIPTION
A. ESTABLISHMENT OF THE ROV MATHEMATICAL MODEL
The kinematic and dynamic model of an ROV must be established under two reference systems: a body-fixed system and an Earth-fixed system, as shown in Fig. 1 [33].

TABLE 1. Units for the magnetic properties.

Parameters of Motion				Parameters of Force	
Name	Parameter	Name	Parameter	Name	Parameter
Surge	x	Surge Speed	u	Surge Force	X
Sway	y	Sway Speed	v	Sway Force	Y
Heave	z	Heave Speed	w	Heave Force	Z
Roll	ϕ	Roll Speed	p	Roll Moment	K
Pitch	θ	Pitch Speed	q	Pitch Moment	M
Yaw	ψ	Yaw Speed	r	Yaw Moment	N

The ROV performs six degrees of freedom in the water, three-axis movement, and three-axis rotation. For ease of calculation, the underwater vehicle motion parameters are defined in Table 1.

The kinematic equation is given by

$$\dot{\eta} = J(\eta) v \qquad (1)$$

where the pose $\eta = [x\ y\ z\ \phi\ \theta\ \psi]^T \in R^6$ contains the global position $\eta_1 = [x\ y\ z]^T$ and Euler angles $\eta_2 = [\phi\ \theta\ \psi]^T$ expressed in the Earth-fixed frame; the velocity vector $v = [u\ v\ w\ p\ q\ r]^T \in R^6$ is composed of the linear velocity vector $v_1 = [u\ v\ w]^T$ and angular velocity vector $v_2 = [p\ q\ r]^T$, both according to the body-fixed frame; and $J(\eta)$ is the transformation matrix between the velocity of the ROV in the body-fixed frame and the pose velocity in the Earth-fixed frame.

The hydrodynamic model is given by [33]

$$M(v)\dot{v} + C(v)v + D(v)v + g(\eta) = \tau + \tau_d \qquad (2)$$

formed by the vectors $v \in R^6$ and $\eta \in R^6$, which are defined above. $M(v) = M_0(v) + \Delta M(v) \in R^{6\times 6}$ is the matrix of inertia, $C(v) = C_0(v) + \Delta C(v) \in R^{6\times 6}$ is the matrix of Coriolis and centripetal terms, and $D(v) = D_0(v) + \Delta D(v) \in R^{6\times 6}$ is the damping matrix. The vector $g(\eta) = g_0(\eta) + \Delta g(\eta) \in R^6$ is the combined force generated by gravity and buoyancy, $\tau \in R^6$ is the force and moment of the ROV under 6 DOFs, and $\tau_d \in R^6$ is the force and moment of external disturbance. $\Delta M(v)$, $\Delta C(v)$, $\Delta D(v)$ and $\Delta g(\eta)$ are the system uncertainties caused by factors such as the mathematical modeling error and parameter measurement error of the ROV.

To facilitate the controller design, the coordinate conversion of the ROV dynamic equation in (2) is as follows (assuming that $J(\eta)$ is nonsingular) [33]:

$$\begin{cases} \dot{\eta} = J(\eta) v \Leftrightarrow v = J^{-1}(\eta)\dot{\eta} \\ \ddot{\eta} = J(\eta)\dot{v} + \dot{J}(\eta) v \Leftrightarrow \dot{v} = J^{-1}(\eta)\left[\ddot{\eta} - \dot{J}(\eta) J^{-1}(\eta)\dot{\eta}\right] \end{cases} \qquad (3)$$

After some calculations, the Earth-fixed expression is given below:

$$M_T(\eta)\ddot{\eta} + C_T(\eta)\dot{\eta} + D_T(\eta)\dot{\eta} + g(\eta) = \tau + \tau_d \qquad (4)$$

with

$$M_T(\eta) = MJ^{-1} + \Delta MJ^{-1}\ddot{\eta} \qquad (5)$$

$$C_T(\eta) = CJ^{-1} + \Delta CJ^{-1} - MJ^{-1}\dot{J}J^{-1} - \Delta MJ^{-1}\dot{J}J^{-1} \qquad (6)$$

$$D_T(\eta) = DJ^{-1} + \Delta DJ^{-1} \qquad (7)$$

Assumption 1: The system uncertainty and external interference of the ROV are time-varying but bounded, and its corresponding first derivative is bounded.

Remark 1: The damping effect is the various forces of water on the ROV, which continuously change with the movement of the ROV in water, so the hydrodynamic damping model of the ROV is difficult to accurately express. The marine environment is often changing and unpredictable, but its energy is limited. Therefore, the disturbance acting on the ship can be considered a finite rate of change of the signal, which is unknown and time-varying but bounded. Then, Assumption 1 is reasonable.

B. FUNDAMENTAL THEORY OF PREDEFINED TIME STABILITY

This section introduces some definitions and lemmas about finite time, fixed time, and predefined time stability. To facilitate the predefined time and accuracy stability analysis, consider the following nonlinear system:

$$\dot{x} = f(x), \quad x(0) = x_0 \qquad (8)$$

where x is the system state vector, the function $f(x) : R^n \rightarrow R^n$ is a continuous and smooth nonlinear function, and x_0 is the initial state of system (8).

Definition 1 [34], [35]: Assuming that system (8) is globally asymptotically stable and any solution of system (8) reaches equilibrium in a finite time, system (8) is said to be globally finite time stable, i.e.,

$$\forall t > T(x_0) : x(x_0) = 0 \qquad (9)$$

where $T(x)$ is the actual convergence time function of system (8).

Definition 2 [36], [37]: Assuming that system (8) can converge to a stable state in a finite time and that the stable time function $T(x_0)$ is globally bounded and independent of the initial state of system (8), system (8) is called a globally fixed time stable system, i.e.,

$$\exists T_{\max} > 0 : \forall x_0 \in R^n, \quad T(x_0) < T_{\max} \qquad (10)$$

where $T_{\max}$ is the estimated value of the convergence time of system (8).

Definition 3 [38], [39]: Suppose that system (8) is stable for a fixed time, and there is an adjustable parameter T_c so

that the actual convergence time of the system $T : \mathbb{R}^n \to \mathbb{R}^n$ satisfies:

$$T(x_0) \leq T_c, \quad \forall x_0 \in \mathbb{R}^n \tag{11}$$

Then, system (8) is called a globally predefined time-stable system.

Lemma 1 [40]: If $x_i \in \mathbb{R}^+$, $0 < p < 1$, $q > 1$ is satisfied, then

$$\sum_{i=1}^{n} x_i^p \geq \left(\sum_{i=1}^{n} x_i\right)^p, \quad \sum_{i=1}^{n} x_i^q \geq n^{1-q} \left(\sum_{i=1}^{n} x_i\right)^q \tag{12}$$

Lemma 2 [30], [37], [41]: Suppose system (8) is stable for a fixed time. Define a continuous positive definite radial unbounded function $V(x) : \mathbb{R}^n \to \mathbb{R}^+$ that satisfies $V(x) = 0$ when $x = 0$, and there are k_1, $k_2 > 0$, $0 < p < 1$, $q > 1$ such that any x satisfies the following inequality:

$$\dot{V}(x) \leq -k_1 V^p(x) - k_2 V^q(x) \tag{13}$$

Then, the convergence time estimation of the system can be calculated by the following formula:

$$T_{\max} = \frac{1}{k_1(1-p)} + \frac{1}{k_2(q-1)} \tag{14}$$

III. MAIN RESULTS

In this section, first, a design method of predefined time control is proposed that can estimate the system convergence time closer to the predefined time parameters according to the dominant term of system state adaptive transformation. Then, a predefined time nonsingular fast terminal sliding mode control law is designed by combining the predefined time control method with NFTSMC. Finally, the stability and the predefined time convergence of the controller are analyzed.

A. DESIGN OF THE PREDEFINED TIME NONSINGULAR FAST TERMINAL SLIDING MODE CONTROLLER

The controller design process is described below.

Theorem 1: Define a continuous positive definite radial unbounded function $V(x) : \mathbb{R}^n \to \mathbb{R}^+$ that satisfies the following:

(1) $V(x) = 0 \Rightarrow x \in M$, where $M \in \mathbb{R}^n$ is a nonempty set.
(2) T_c is an adjustable parameter predefined by the user.
(3) For $\forall V(x) > 0$, there are k_1, $k_2 > 0$, $0 < p_2 < 1$, and $q_2 > 1$ such that

$$\dot{V} \leq -\frac{C_v}{T_c}\left(k_1 V^{p_2} + k_2 V^{q_2}\right) \tag{15}$$

where

$$\begin{cases} C_v = \dfrac{1}{k_2^{\frac{1}{q_2}}} \dfrac{1}{1-q_2} k_2^{\frac{1-q_2}{q_2}} & 0 < V(x) < 1 \\[3mm] C_v = \dfrac{1}{k_1^{\frac{1}{p_2}}} \dfrac{2^{(p_2-1)}}{1-p_2} k_1^{\frac{1-p_2}{p_2}} & V(x) > 1 \end{cases} \tag{16}$$

Then, system (8) is stable within the predetermined time, and the convergence time is T_c.

Remark 2: Fixed-time stability makes it difficult to find the explicit relationship between system parameters and the system stability time, which leads to inaccurate estimation of the convergence time, difficult adjustment, and unpredictability. The predetermined time stability solves these problems well and facilitates a direct relationship between system gain and convergence time estimation. The scheduled time stability is a special kind of fixed time stability. Therefore, the convergence time estimation of the predetermined time stability is independent of the initial value and only related to the predetermined parameters C_v.

Remark 3: Equation (15) shows that the control law adapts to the system state. When the system state is far from the equilibrium point, fast convergence is achieved by the nonlinear term $\dot{V}(x) \leq -k_2 V^{q_2}(x)$. When the system state approaches the equilibrium point, fast convergence is achieved by the nonlinear term $\dot{V}(x) \leq -k_1 V^{p_2}(x)$, and C_v also switches with the system state to ensure that the system can converge within a predetermined time T_c.

The trajectory tracking errors are defined as

$$e = \eta - \eta_d \tag{17}$$

where $\eta_d \in R^6$ is the desired trajectory.

At this point, the first- and second-time derivatives of (17) can be computed, which yields:

$$\dot{e} = \dot{\eta} - \dot{\eta}_d \tag{18}$$

$$\ddot{e} = \ddot{\eta} - \ddot{\eta}_d = M_T^{-1}\left(\tau - C_T(\eta)\dot{\eta} - D_T(\eta)\dot{\eta} - g\right) - \ddot{\eta}_d \tag{19}$$

To further improve the convergence performance of the system state and realize fast convergence of the system state using different dominant terms when it is far from the equilibrium point and close to the equilibrium point while completely solving the singularity problem of the traditional terminal sliding mode, the following improved NFTSMC sliding surface is proposed:

$$s = e + \frac{1}{\alpha}|e|^{p_1}\operatorname{sgn}(e) + \frac{1}{\beta}|\dot{e}|^{q_1}\operatorname{sgn}(\dot{e}) \tag{20}$$

where $s = [s_1 \ s_2 \ \cdots \ s_6]^T$ is the sliding mode vector, α, $\beta \in \mathbb{R}^+$, $p_1 > 1$ and $0 < q_1 < 1$. The use of $|e|$ and $|\dot{e}|$ in the slide surface in (20) instead of e and $\dot{e}$ in the conventional terminal slide completely solves the problem of singularity in the terminal slide.

The derivative of the sliding surface in (20) can be calculated as follows:

$$\dot{s} = \dot{e} + \frac{p_1}{\alpha}|e|^{p_1-1}\dot{e} + \frac{q_1}{\beta}|\dot{e}|^{q_1-1}\ddot{e} \tag{21}$$

Combining Lemma 3 with the above sliding surface in (20), the proposed PTNFTSMC can be expressed as follows:

$$\tau = M_T\left\{\frac{\beta}{q_1}|\dot{e}|^{1-q_1}\left[-\frac{C_v}{T_c}\left(\frac{k_1}{2^{p_2}}s^{2p_2-1} + \frac{k_2}{2^{q_2}}s^{2q_2-1}\right)\operatorname{sgn}(s)\right.\right.$$
$$\left.\left.-\dot{e} - \frac{p_1}{\alpha}|e|^{p_1-1}\dot{e}\right] + \ddot{\eta}_d\right\} + C_T(\eta)\dot{\eta} + D_T(\eta)\dot{\eta} + g \tag{22}$$

The control block diagram of PTNFTSMC proposed by (17)-(22) is shown in Fig. 2. To avoid singularity problems in the control output, the parameter selection range of (15) is narrowed to $0.5 \leq p_2 < 1$, and $\{q_2 | q_2 = 2n + 1, n \in N^+\}$.

Remark 4: In practical applications, the chattering phenomenon of PTNFTSMC can be improved by some common methods to suppress chattering, such as the replacement saturation function method.

B. PROOF OF CONTROLLER STABILITY AND PREDEFINED TIME CONVERGENCE

The Lyapunov function V is constructed as follows:

$$V = \frac{1}{2}s^2 \tag{23}$$

The Lyapunov function V satisfies $V \geq 0$, $s \in \mathbb{R}^n$. Combined with (21), the first derivative of the function in (23) can be calculated as follows:

$$
\begin{aligned}
\dot{V} &= s\dot{s} \\
&= s\left(\dot{e} + \frac{p_1}{\alpha}|e|^{p_1-1}\dot{e} + \frac{q_1}{\beta}|\dot{e}|^{q_1-1}\ddot{e}\right) \\
&= s\left\{\dot{e} + \frac{p_1}{\alpha}|e|^{p_1-1}\dot{e} + \frac{q_1}{\beta}|\dot{e}|^{q_1-1}\right. \\
&\quad \left.\left[M_T^{-1}\left(\tau - C_T(\eta)\dot{\eta} - D_T(\eta)\dot{\eta} - g\right) - \ddot{\eta}_d\right]\right\}
\end{aligned} \tag{24}
$$

By substituting the designed predefined time nonsingular fast terminal sliding mode control law in (22) into (24), the first derivative of the Lyapunov function $\dot{V}$ can be obtained as follows:

$$\dot{V} \leq -\frac{C_v}{T_c}\left(k_1 V^{p_2} + k_2 V^{q_2}\right) \tag{25}$$

The first derivative of the Lyapunov function $\dot{V}$ satisfies $\dot{V} \leq 0$. According to the Lyapunov stability principle, the function in (23) is positive definite, and the derivative in (25) is negative definite. Therefore, the proposed PTNFTSMC is asymptotically stable. The controller stability is proved.

From (25), we have

$$-\frac{T_c}{C_v}\frac{1}{(k_1 V^{p_2} + k_2 V^{q_2})}dV \geq dt \tag{26}$$

Integrating (26) from $t = T(x_0)$ yields

$$T(x_0) = \int_0^{T(x_0)} dt \leq -\int_{V(x_0)}^0 \frac{T_c}{C_v}\frac{1}{(k_1 V^{p_2} + k_2 V^{q_2})}dV \tag{27}$$

As shown in (16), the control parameters in the predefined time controller presented in this paper will be dynamically adjusted as the system state changes to adjust the convergence dominant term according to the system state. To facilitate the convergence analysis of the controller in a predetermined time, the system state is divided into two parts: far away from

the equilibrium point and near the equilibrium point, so (27) can be rewritten as follows:

$$
\begin{aligned}
T(x_0) &\leq -\int_{V(x_0)}^0 \frac{T_c}{C_v}\frac{1}{(k_1 V^{p_2} + k_2 V^{q_2})}dV \\
&= \int_{V(x_1)}^{V(x_0)} \frac{T_{c1}}{C_{v1}}\frac{1}{(k_1 V^{p_2} + k_2 V^{q_2})}dV \\
&\quad + \int_0^{V(x_1)} \frac{T_{c2}}{C_{v2}}\frac{1}{(k_1 V^{p_2} + k_2 V^{q_2})}dV
\end{aligned} \tag{28}
$$

where T_{c1} is the estimation of the convergence time required for the system state to go from far away to near the equilibrium point, T_{c2} is the estimation of the convergence time required for the system state to go from near the equilibrium point to system stability, and x_1 is a system state close to the equilibrium point, which satisfies $0 < V(x_1) < 1$. The time convergence analysis of the two convergence processes is as follows:

1) SYSTEM STATE FAR FROM THE EQUILIBRIUM POINT

From (28), we have

$$
\begin{aligned}
T_1(x_0) &\leq \int_{V(x_1)}^{V(x_0)} \frac{T_{c1}}{C_{v1}}\frac{1}{(k_1 V^{p_2} + k_2 V^{q_2})}dV \\
&\leq \int_{V(x_1)}^{V(x_0)} \frac{T_{c1}}{C_{v1}}\frac{1}{k_1 V^{p_2}}dV
\end{aligned} \tag{29}
$$

where $T_1(x_0)$ is the actual convergence time required for the system state to go from far away to near the equilibrium point. Since $P_2 > 1$, according to Lemma 1, we have

$$
\begin{aligned}
&\int_{V(x_1)}^{V(x_0)} \frac{T_{c1}}{C_{v1}}\frac{1}{k_1 V^{p_2}}dV \\
&\leq \left. \frac{T_{c1}}{C_{v1}}\frac{1}{k_1^{\frac{1}{p_2}}}\frac{2^{(p_2-1)}}{1-p_2}\left(k_1^{\frac{1}{p_2}}V\right)^{1-p_2} \right|_{V(x_1)}^{V(x_0)} \\
&= \frac{T_{c1}}{C_{v1}}\frac{1}{k_1^{\frac{1}{p_2}}}\frac{2^{(p_2-1)}}{1-p_2}k_1^{\frac{1-p_2}{p_2}}\left(V^{1-p_2}(x_0) - V^{1-p_2}(x_1)\right)
\end{aligned} \tag{30}
$$

If $V(x_0) \to \infty$, since $0 < V(x_1) < 1$, we have

$$
\begin{aligned}
T_1(x_0) &\leq \int_{V(x_1)}^{V(x_0)} \frac{T_{c1}}{C_{v1}}\frac{1}{k_1 V^{p_2}}dV \\
&\leq \frac{T_{c1}}{C_{v1}}\frac{1}{k_1^{\frac{1}{p_2}}}\frac{2^{(p_2-1)}}{1-p_2}k_1^{\frac{1-p_2}{p_2}} = T_{c1}
\end{aligned} \tag{31}
$$

2) SYSTEM STATE APPROACHING THE EQUILIBRIUM POINT

From (28), we have

$$
\begin{aligned}
T_2(x_0) &\leq \int_0^{V(x_1)} \frac{T_{c2}}{C_{v2}}\frac{1}{(k_1 V^{p_2} + k_2 V^{q_2})}dV \\
&\leq \int_0^{V(x_1)} \frac{T_{c2}}{C_{v2}}\frac{1}{k_2 V^{q_2}}dV
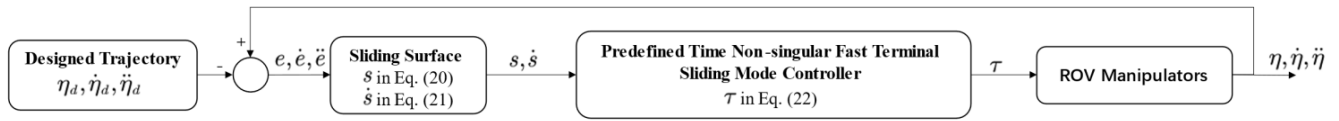\end{aligned} \tag{32}
$$

FIGURE 2. Block diagram of PTNFTSMC.

where $T_2(x_0)$ is the actual convergence time required for the system state to go from approaching the equilibrium point to system stability. Since $0 < q_2 < 1$, according to Lemma 1, we have

$$
\int_0^{V(x_1)} \frac{T_{c2}}{C_{v2}} \frac{1}{k_2 V^{q_2}} dV
$$

$$
\leq \frac{T_{c2}}{C_{v2}} \frac{1}{k_2^{\frac{1}{q_2}}} \frac{1}{1-q_2} \left(k_2^{\frac{1}{q_2}} V \right)^{1-q_2} \Bigg|_0^{V(x_1)}
$$

$$
= \frac{T_{c2}}{C_{v2}} \frac{1}{k_2^{\frac{1}{q_2}}} \frac{1}{1-q_2} k_2^{\frac{1-q_2}{q_2}} V^{1-q_2}(x_1) \tag{33}
$$

Since $0 < V(x_1) < 1$ and $0 < q_2 < 1$, we have

$$
T_2(x_0) \leq \int_0^{V(x_1)} \frac{T_{c2}}{C_{v2}} \frac{1}{k_2 V^{q_2}} dV
$$

$$
\leq \frac{T_{c2}}{C_{v2}} \frac{1}{k_2^{\frac{1}{q_2}}} \frac{1}{1-q_2} k_2^{\frac{1-q_2}{q_2}} = T_{c2} \tag{34}
$$

From the analysis of (26)-(34), it can be seen that

$$
T(x_0) = T_1(x_0) + T_2(x_0) \leq T_{c1} + T_{c2} = T_c \tag{35}
$$

Therefore, the proposed PTNFTSMC is predefined as time-stable. The proof is complete.

Remark 5: When the initial state of the system is close to the system equilibrium point, the controller does not change the system state from far away from the equilibrium point to near the equilibrium point through the control law, so $T(x_0) \leq T_c = T_{c2}$. As the proof is the same, it will not be repeated here.

IV. SIMULATION RESULTS

In this section, to verify the convergence, adjustability, and high accuracy of the predefined time of the proposed PTN-FTSMC control scheme, mathematical simulation comparative experiments are carried out. The experiment is mainly divided into three parts: (1) Under the same predefined time parameters, the system conducts comparative experiments on systems under different initial states. (2) The system uses different predefined time parameters for comparative experiments under the same initial state. (3) The system is tested under different controllers. The first two mainly verify the accuracy of the predefined time convergence of the proposed PTNFTSMC. The third part compares different controllers to verify the advantages of the proposed PTNFTSMC in predefined time convergence and error control. The structural parameters of the ROV used in the experiment are shown in

TABLE 2. ROV structural parameters.

Parameter	Value	Parameter	Value
m	11.5	X_G	0
B	114.8	Y_G	0
W	112.8	Z_G	0
I_x	0.16	X_B	0
I_y	0.16	Y_B	0
I_z	0.16	Z_B	0.02

TABLE 3. ROV additional mass and hydrodynamic coefficient.

Parameter	Value	Parameter	Value	Parameter	Value
X_u	-4.03	$X_{u\|u\|}$	-18.18	$K_{\dot{p}}$	-0.12
Y_v	-6.22	$Y_{v\|v\|}$	-21.66	$M_{\dot{q}}$	-0.12
Z_w	-5.18	$Z_{w\|w\|}$	-36.99	$N_{\dot{r}}$	-0.12
$X_{\dot{u}}$	-5.5	K_p	-0.07	$K_{p\|p\|}$	-1.55
$Y_{\dot{v}}$	-12.7	M_q	-0.07	$M_{q\|q\|}$	-1.55
$Z_{\dot{w}}$	-14.57	N_r	-0.07	$N_{r\|r\|}$	-1.55

Table 2, and the added mass and hydrodynamic coefficient are shown in Table 3.

To ensure the unity of simulation experiments, all experiments use the same controller parameters and the same ROV target trajectory. Except for the predefined time parameter T_c, the other parameters of PTNFTSMC in all simulation experiments are set as follows: $\alpha = 76$, $\beta = 11.5$, $p_1 = 3$, $q_1 = 0.5$, $k_1 = 0.4$, $k_2 = 0.1$, $p_2 = 1.5$ and $q_2 = 0.5$. The desired trajectory of the ROV is designed to track the following spiral:

$$
\begin{cases}
x_d = 5\cos(0.05\pi t) + 5 \\
y_d = 5\sin(0.05\pi t) + 5 \\
z_d = -0.25t \\
\phi_d = t \\
\theta_d = t \\
\psi_d = -0.25
\end{cases} \tag{36}
$$

A. SIMULATION ANALYSIS OF THE PREDEFINED TIME CONVERGENCE OF PTNFTSMC

In this subsection, to verify the convergence of the proposed PTNFTSMC within the predefined time, several groups of different system initial states are set under the condition of a fixed predefined time parameter $T_c = 10s$, as shown in Table 4.
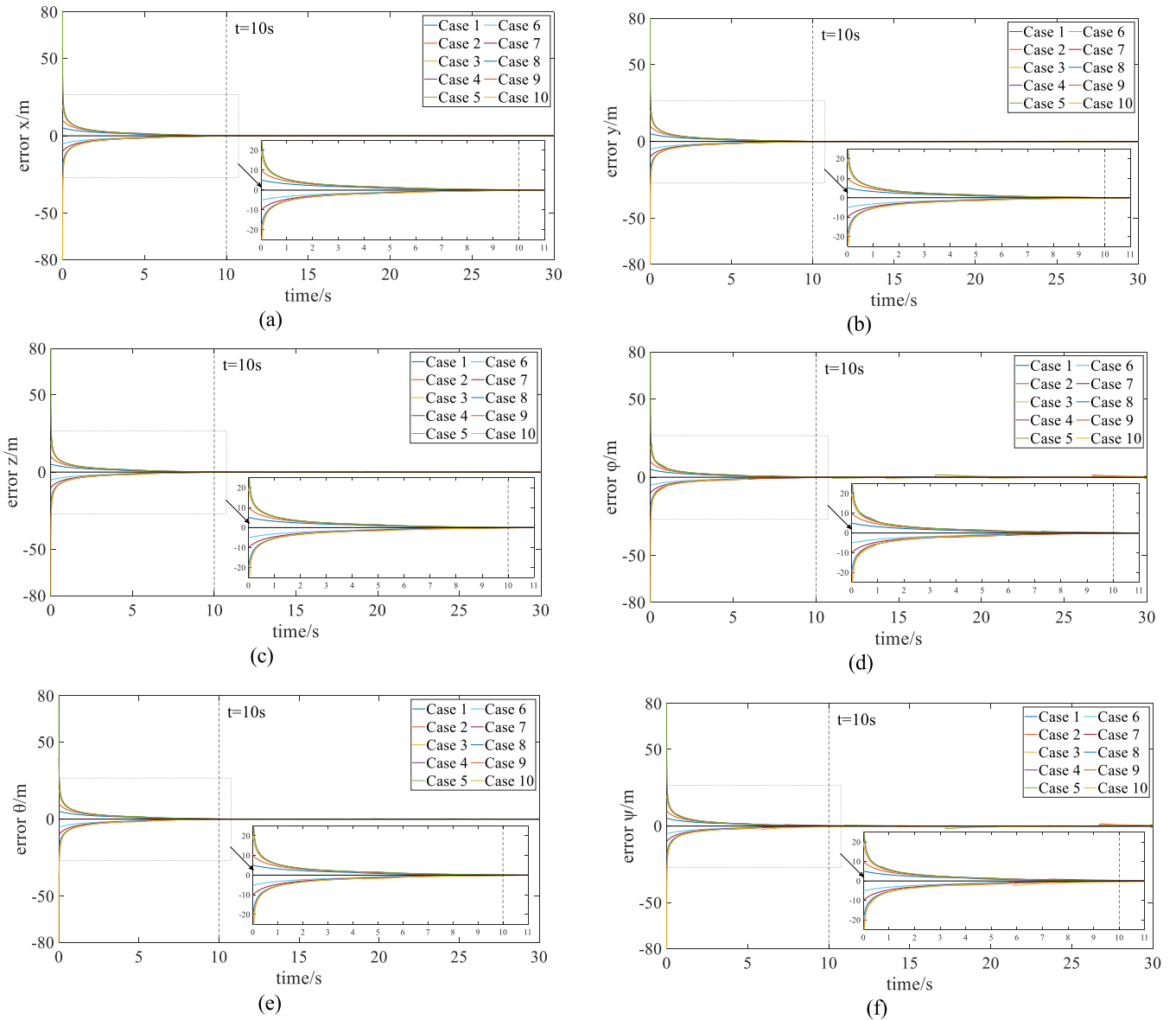
FIGURE 3. Error convergence trajectories of the ROV under different initial states of the system.

TABLE 4. ROV system initial states.

	x_0	y_0	z_0	ϕ_0	θ_0	ψ_0
Case 1	15	10	5	5	5	4.75
Case 2	20	15	10	10	10	9.75
Case 3	30	25	20	20	20	19.75
Case 4	50	45	40	40	40	39.75
Case 5	90	80	80	80	80	79.75
Case 6	5	0	-5	-5	-5	-5.25
Case 7	0	-5	-10	-10	-10	-10.25
Case 8	-10	-15	-20	-20	-20	-20.25
Case 9	-30	-35	-40	-40	-40	-40.25
Case 10	-70	-75	-80	-80	-80	-80.25

In the initial states of different systems, the trajectory tracking errors of the ROV for various degrees of freedom are shown in Fig. 3.

Figure 3 shows that when the predefined parameter of PTNFTSMC is set to $T_c = 10s$, under different initial states of the system, the errors of each degree of freedom of the ROV can converge in approximately 10 s, and the actual convergence time is very close to the preset time parameter T_c. At the same time, after the controller converges, the system error is controlled within a very small fraction. In summary, the stability and predefined time convergence of the proposed PTNFTSMC are verified.

B. SIMULATION ANALYSIS OF THE PREDEFINED TIME ADJUSTABILITY OF PTNFTSMC

In this subsection, to verify the predefined time adjustability of the proposed PTNFTSMC, several groups of different predefined time parameters are set under the same initial state
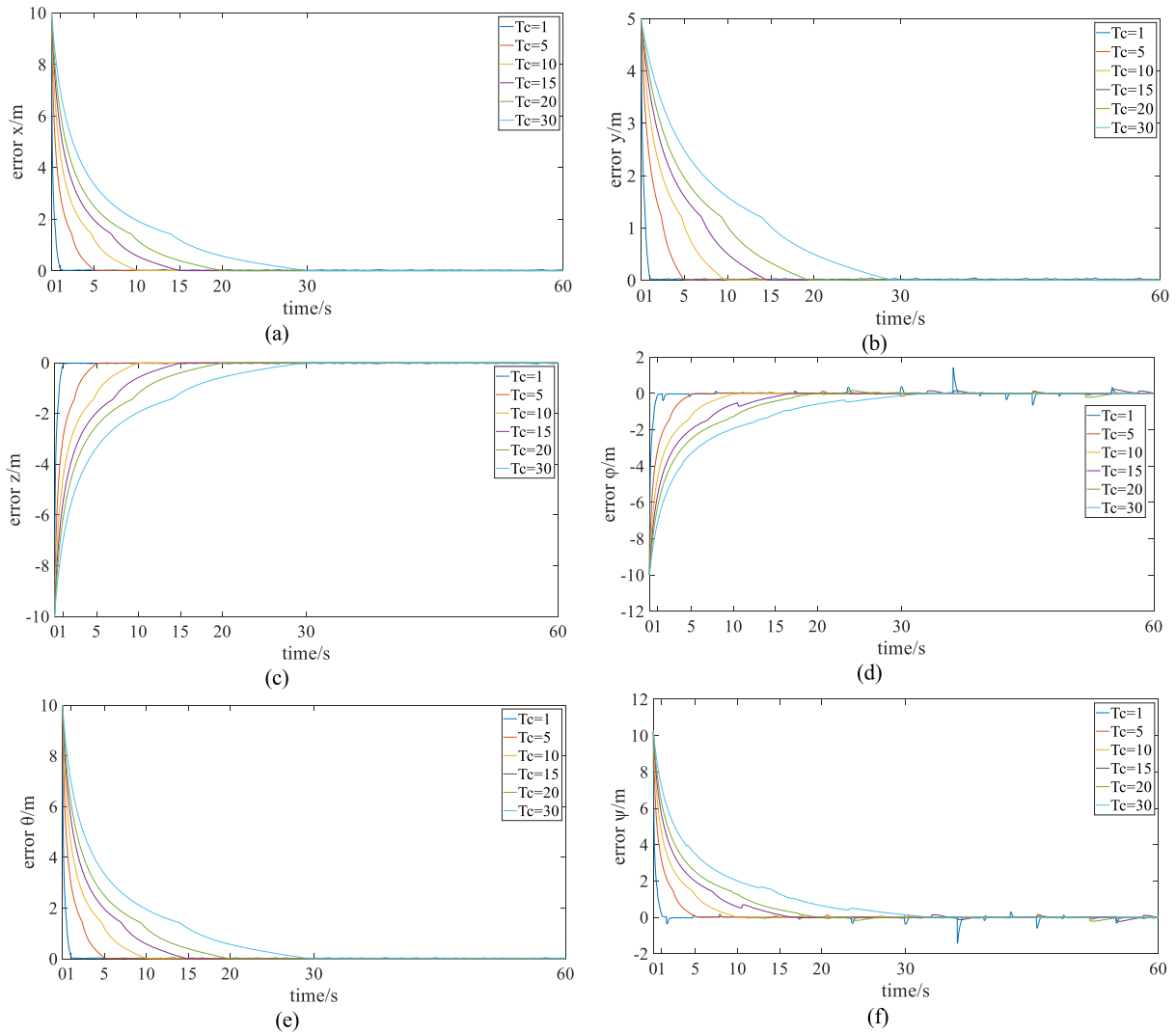
FIGURE 4. Error convergence trajectories of the ROV for different predefined time parameters.
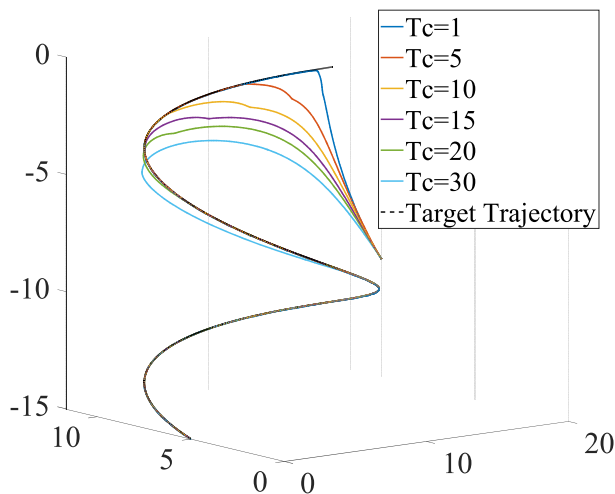

FIGURE 5. The three-dimensional trajectory of the ROV for different predefined time parameters.

of the system as follows: $T_c = 1s$, $T_c = 5s$, $T_c = 10s$, $T_c = 15s$, $T_c = 20s$ and $T_c = 30s$. The initial state of the system

is set to $x_0 = [20, 10, -10, -10, 10, 10]$. Under different predefined time parameters, the ROV trajectory tracking error of each degree of freedom is shown in Fig. 4, and the three-dimensional trajectory of the ROV is shown in Fig. 5.

Combining Fig. 4 and Fig. 5, it can be seen that the actual convergence time of the ROV changes dynamically with the predefined time parameter T_c, and the actual convergence time of the system almost sums up with the predefined time. In summary, the actual convergence time of the proposed PTNFTSMC depends on the predefined time parameter T_c, which verifies the predefined time adjustability of PTNFTSMC.

C. COMPARATIVE SIMULATION ANALYSIS OF PTNFTSMC AND OTHER EXISTING CONTROL SCHEMES

In this subsection, the PTNFTSMC proposed in this paper, the nonsingular terminal sliding mode control (NFTSMC) in [42], the fixed time sliding mode control (FTSMC) in [43] and the predefined time sliding mode control (PTSMC)
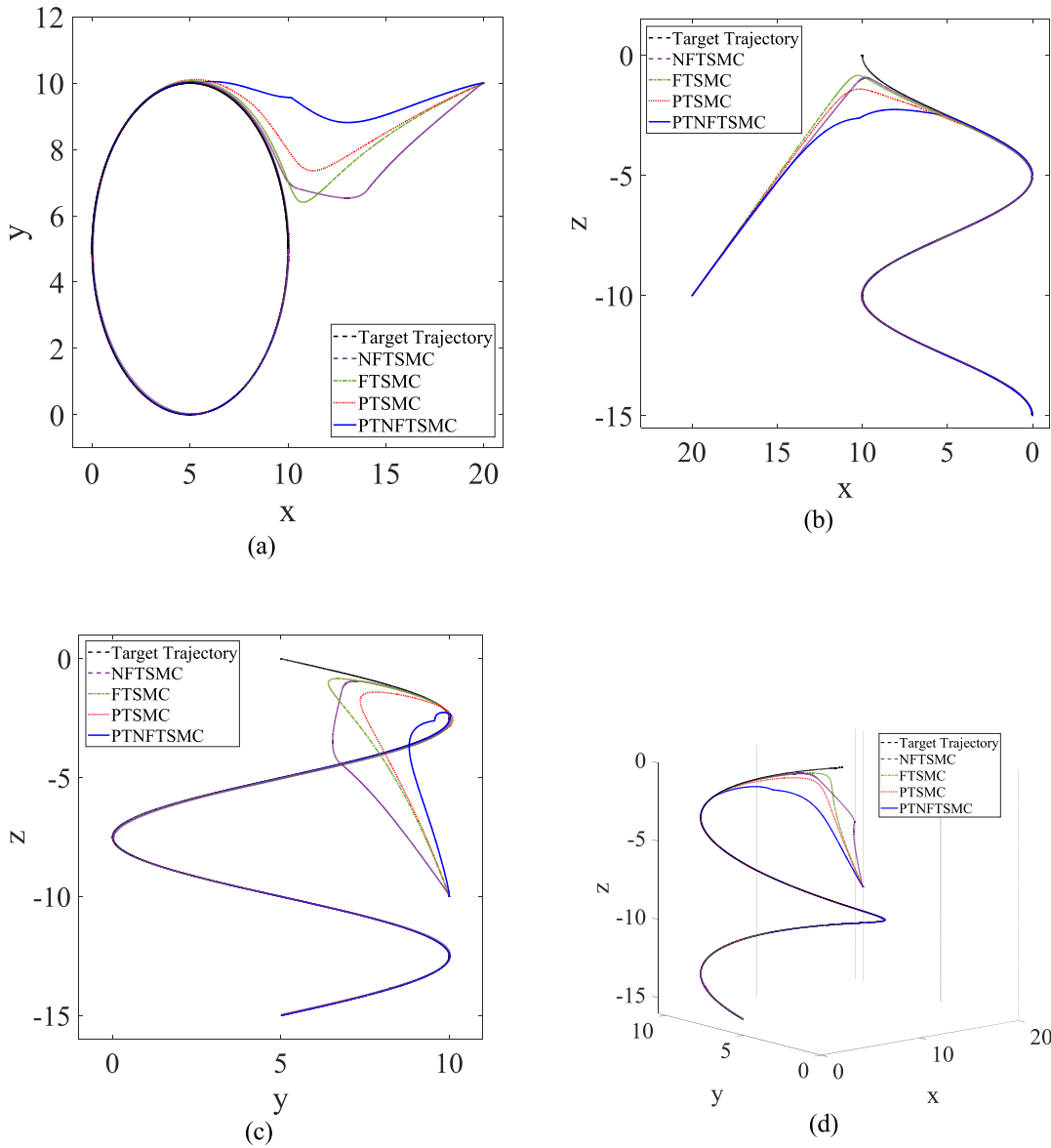
FIGURE 6. The actual and target trajectories of four different controllers.

in [30] are compared and simulated to prove the superiority of the proposed method.

The control law of NFTSMC is designed as follows:

$$\tau = M_T \left[\frac{\beta}{q} |\dot{e}|^{1-q} \left(-k_1 s - k_2 sign\,(s) - \dot{e} - \frac{p}{\alpha} |e|^{p-1} \dot{e} \right) + \ddot{\eta}_d \right] + C_T\,(\eta)\,\dot{\eta} + D_T\,(\eta)\,\dot{\eta} + g$$

where $s = e + \frac{1}{\alpha} |e|^p\,sign\,(e) + \frac{1}{\beta} |\dot{e}|^q\,sign\,(\dot{e})$, $p > 1$, $0 < q < 1$, and k_1, k_2, α and β are positive constants.

The control law of FTSMC is designed as follows:

$$\tau = M_T \left[-\left(\frac{1}{2^p} s^{2p-1} + \frac{1}{2^q} s^{2q-1} \right) sign\,(s) + \ddot{\eta}_d - c\dot{e} \right] + C_T\,(\eta)\,\dot{\eta} + D_T\,(\eta)\,\dot{\eta} + g \quad (37)$$

where $s = ce + \dot{e}$, $p > 1$, $0 < q < 1$, and c is a positive constant. The estimation of the controller convergence time can be calculated as follows:

$$T = \frac{2}{(p-1)} + \frac{2}{(1-q)} \quad (38)$$

The control law of PTSMC is designed as follows:

$$\tau = M_T \left[-\frac{C_v}{T_c} \left(\frac{\alpha}{2^p} s^{2p-1} + \frac{\beta}{2^q} s^{2q-1} \right) sign\,(s) + \ddot{\eta}_d - c\dot{e} \right] + C_T\,(\eta)\,\dot{\eta} + D_T\,(\eta)\,\dot{\eta} + g \quad (39)$$

where $s = ce + \dot{e}$, $p > 1$, $0 < q < 1$, α, β and c are positive constants, T_c is a predefined time parameter and the expression of CV is the same as (16).

To compare the fairness and rationality of the simulation experiment, the parameters of the three control algorithms
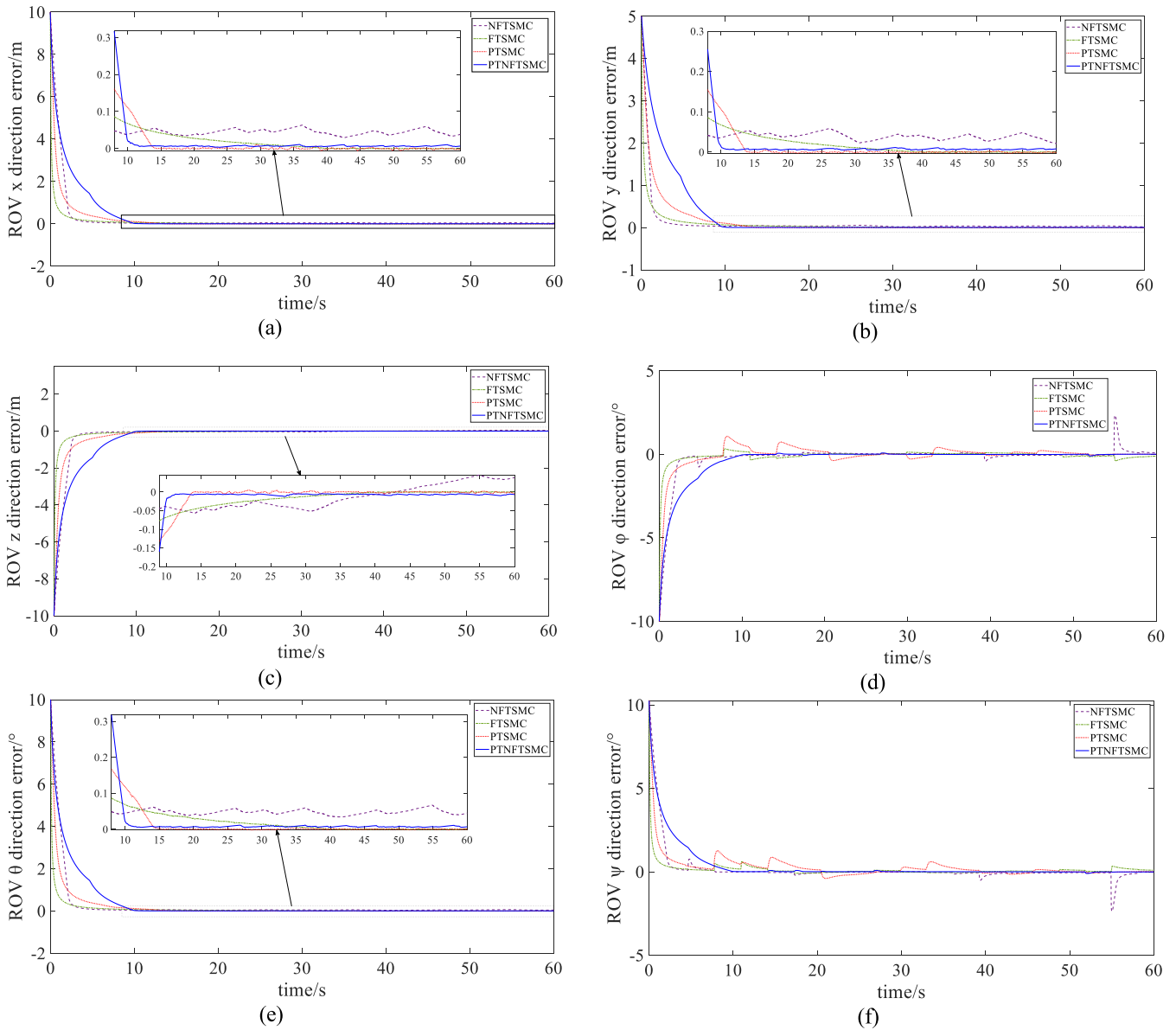
FIGURE 7. The control errors of the four controllers in each degree of freedom.

TABLE 5. Control parameters of the three different controls.

Control Methods	Parameters	Value
NFTSMC	α , β , p , q , k_1 , k_2	7, 2, 3, 0.5, 2, 5
FTSMC	p , q , c	1.5, 0.5, 50
PTSMC	α , β , p , q , c	0.5, 0.2, 1.5, 0.5, 5,10
PTNFTSMC	α , β , p_1 , q_1 , p_2 , q_2 , k_1 , k_2 , T_c	76, 11.5, 3, 0.5, 1.5, 0.5, 0.4, 0.1,10

used for comparison refer to the parameters used in the original text and are adjusted according to the actual simulation results of the ROV in this paper to ensure that each control scheme can achieve a better control effect. The parameters of each control instrument are shown in Table 5.

The comparative simulation results of the four control schemes are shown in Figs. 6-8. Fig. 6 shows the actual trajectory and target trajectory of the ROV under the action of four different controllers; Fig. 7 shows the control errors of the four different controllers in each degree of freedom; and Fig. 8 shows the control forces and moments of the four different controllers in each degree of freedom.

By analyzing the simulation results in Figs. 6-8, the following conclusions can be drawn.

1) COMPARATIVE ANALYSIS WITH NFTSMC

As seen from Fig. 7, the tracking error convergence accuracy of NFTSMC is the worst among all compared control algorithms. There are obvious error fluctuations after convergence, and at approximately 55 s, NFTSMC exhibits the largest error fluctuations among the four control schemes. Compared with NFTSMC, the proposed
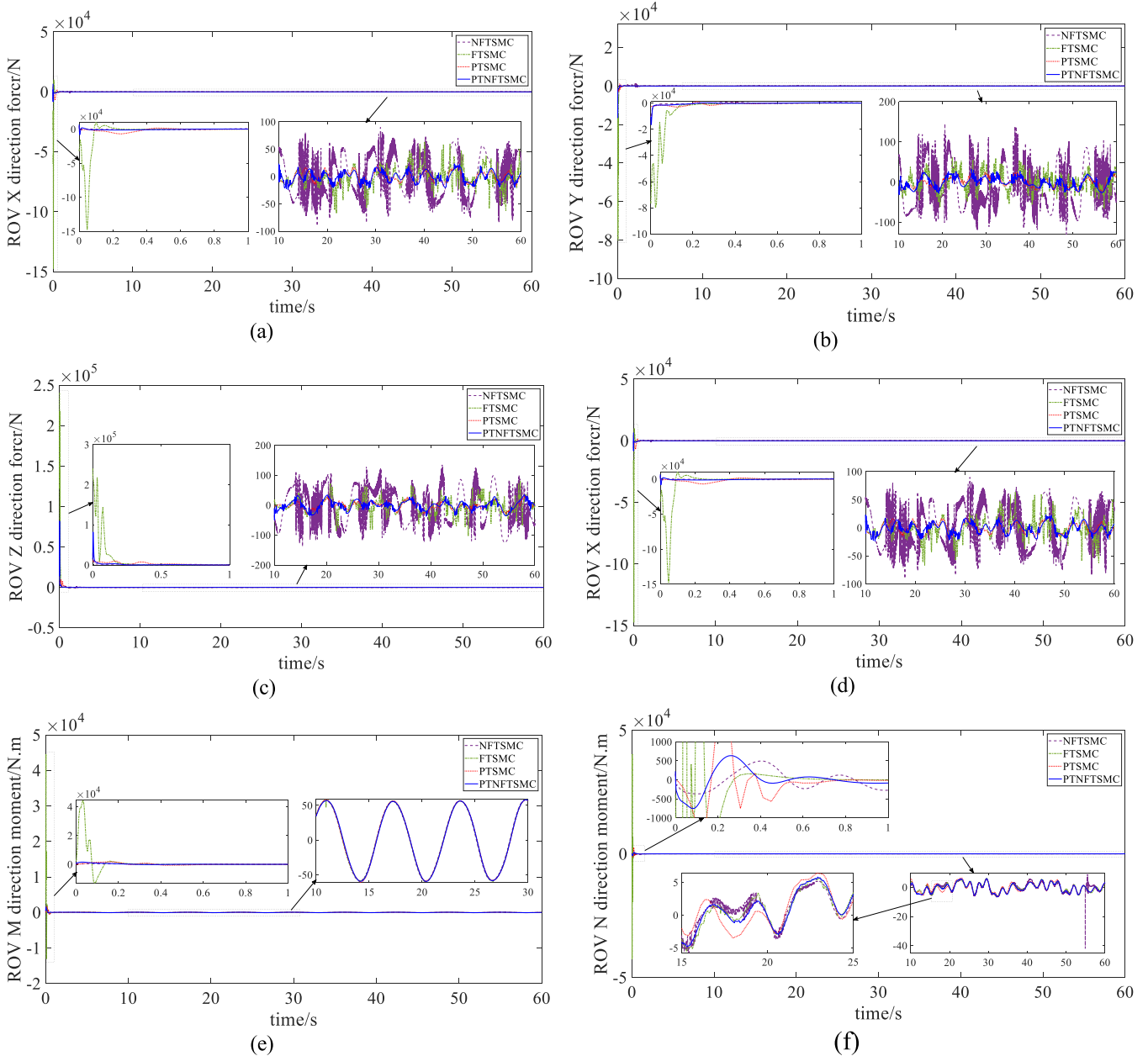
FIGURE 8. Control forces and moments of the four different controllers for each degree of freedom.

PTNFTSMC improves the system tracking error accuracy by approximately two orders of magnitude, and PTNFTSMC significantly outperforms the other control schemes in terms of error fluctuation suppression. In addition, it can be seen from Fig. 8 that the control output of NFTSMC shows a significant chattering phenomenon. Compared with NFTSMC, although the control output of PTNFTSMC still has a chattering phenomenon due to the absence of the chattering suppression term, PTNFTSMC can reasonably allocate the energy consumption by adjusting the convergence time and effectively reducing the amplitude and frequency of output chattering. Most importantly, NFTSMC exhibits finite time convergence, but its convergence time depends on the initial

state of the system, which is detrimental to the ROV to complete the position adjustment within the specified time.

2) COMPARATIVE ANALYSIS WITH FTSMC AND PTSMC
FTSMC achieves the convergence of the system in a fixed time range under different initial states, but the convergence time estimate of FTSMC is too conservative. The convergence time of FTSMC is estimated to be 8 s by (38), but it can be seen from Fig. 7 that FTSMC controls the error within a smaller range of approximately 3 s. In general, we always hope that the actual convergence time of the system tracking error is closer to the predefined convergence time set, which will facilitate the reasonable setting of the

system convergence time because a faster convergence time often means more energy consumption. As seen in Fig. 7, the faster convergence of FTSMC leads to a great initial control output within approximately 0.3 s at the beginning of system operation. Due to the introduction of the predefined time design method, PTSMC exhibits a significant improvement in the tunability and estimation accuracy of the convergence time compared with FTSMC, but because PTSMC adopts the sliding mode control strategy, the sliding mode control has the problem of a slow convergence speed, which leads to the actual convergence time of PTSMC being larger than the predefined convergence time. As seen from Fig. 7, the actual convergence time of PTSMC is approximately 14 s for a predefined time $T_c = 10s$. Meanwhile, a similar problem exists for FTSMC, which needs approximately 40 s to achieve a more desirable convergence effect.

The proposed PTNFTSMC effectively combines the advantages of predefined time control and NFTSMC. Combining Fig. 4 and Fig. 7, it can be seen that PTNFTSMC uses different dominant terms when the system state is far from the equilibrium point and close to the equilibrium point, which makes PTNFTSMC switch to another dominant term when the convergence rate of one dominant term tends to level off, ensuring fast and stable convergence of PTNFTSMC in different system states. As seen from Fig. 7, compared with those of FTSMC and PTSMC, the actual convergence time of PTNFTSMC in each degree of freedom is approximately 10 s, which is very close to the predetermined convergence time, and the error of the converged system is stable and the error fluctuation is the smallest among the four control schemes.

In summary, the proposed PTNFTSMC scheme has better convergence accuracy and smaller control output amplitude and chattering than NFTSMC and has predefined time convergence characteristics, and its actual convergence time is closer to the predefined convergence time than those of FTSMC and PTSMC, which is more conducive to the reasonable setting of the system convergence time.

V. CONCLUSION

In this paper, a new predefined time-nonsingular fast terminal sliding mode control method is proposed for the tracking control of a 6-degrees-of-freedom ROV. First, a simplified design method for a predefined-time controller is proposed. Then, predefined-time nonsingular fast terminal sliding-mode control is developed by combining the proposed design method with a nonsingular fast terminal sliding-mode surface. It is rigorously demonstrated that the actual convergence time of the tracking error in the proposed control method is independent of the initial state of the system and can be set with a prescribed time parameter. Finally, simulation comparison experiments show that the proposed control scheme has more accurate convergence time estimation, higher convergence accuracy, and more stable control results compared with existing control schemes, which demonstrates the superiority of the proposed scheme. The next target is to solve the

chattering problem of the proposed PTNFTSMC and apply it to a real ROV.

REFERENCES

[1] N. Xue, "Research on motion control system of remote operated vehicle," M.S. thesis, School Civil Eng. Transp., South China Univ. Technol., Guangdong, China, 2020, doi: 10.27151/d.cnki.ghnlu.2020.002940.

[2] J. Teague, M. J. Allen, and T. B. Scott, "The potential of low-cost ROV for use in deep-sea mineral, ore prospecting and monitoring," *Ocean Eng.*, vol. 147, pp. 333–339, Jan. 2018.

[3] M. Yang, Z. Sheng, G. Yin, and H. Wang, "A recurrent neural network based fuzzy sliding mode control for 4-DOF ROV movements," *Ocean Eng.*, vol. 256, Jul. 2022, Art. no. 111509.

[4] S. Soylu, A. A. Proctor, R. P. Podhorodeski, C. Bradley, and B. J. Buckham, "Precise trajectory control for an inspection class ROV," *Ocean Eng.*, vol. 111, no. 1, pp. 508–523, Jan. 2016.

[5] S. A. Gayvoronskiy, T. Ezangina, and I. Khozhaev, "Providing a robust aperiodic transient process in motion control system unmanned underwater vehicle with interval parameters," *IFAC-PapersOnLine*, vol. 51, no. 29, pp. 220–225, 2018.

[6] Z. A. Ali, X. Li, and M. A. Tanveer, "Controlling and stabilizing the position of remotely operated underwater vehicle equipped with a gripper," *Wireless Personal Commun.*, vol. 116, no. 2, pp. 1107–1122, 2019.

[7] P. N. N. Thanh, P. M. Tam, and H. P. H. Anh, "A new approach for three-dimensional trajectory tracking control of under-actuated AUVs with model uncertainties," *Ocean Eng.*, vol. 228, May 2021, Art. no. 108951.

[8] Y. Wang, M. Zhang, P. A. Wilson, and X. Liu, "Adaptive neural network-based backstepping fault tolerant control for underwater vehicles with thruster fault," *Ocean Eng.*, vol. 110, pp. 15–24, Dec. 2015.

[9] H. Zhou, Z. Wei, Z. Zeng, C. Yu, and L. Lian, "Adaptive robust sliding mode control of autonomous underwater glider with input constraints for persistent virtual mooring," *Appl. Ocean Res.*, vol. 95, Feb. 2020, Art. no. 102027.

[10] Y. Zhong and F. Yang, "Dynamic modeling and adaptive fuzzy sliding mode control for multi-link underwater manipulators," *Ocean Eng.*, vol. 187, Sep. 2019, Art. no. 106202.

[11] B. Xu, L. Zhang, and W. Ji, "Improved non-singular fast terminal sliding mode control with disturbance observer for PMSM drives," *IEEE Trans. Transport. Electrific.*, vol. 7, no. 4, pp. 62–2753, Dec. 2021.

[12] Q. Hou, S. Ding, X. Yu, and K. Mei, "A super-twisting-like fractional controller for SPMSM drive system," *IEEE Trans. Ind. Electron.*, vol. 69, no. 9, pp. 84–9376, Sep. 2022.

[13] C. Yuan, R. Zhang, X. Zhao, and J. Gao, "Adaptive fuzzy inverse trajectory tracking control of underactuated underwater vehicle with uncertainties," *Ocean Eng.*, vol. 121, pp. 123–133, Jul. 2016.

[14] X. Huo, T. Ge, and X. Wang, "Horizontal path-following control for deep-sea work-class ROVs based on a fuzzy logic system," *Ships Offshore Struct.*, vol. 13, no. 6, pp. 637–648, Aug. 2018.

[15] P. S. Londhe, S. Mohan, and B. M. Patre, "Robust task-space control of an autonomous underwater vehicle-manipulator system by PID-like fuzzy control scheme with disturbance estimator," *Ocean Eng.*, vol. 139, pp. 1–13, Apr. 2017.

[16] X. Du, D. Chen, and Z. Yan, "Research on control method of unmanned underwater vehicle dynamic positioning based on energy consumption optimization," *Int. J. Adv. Robotic Syst.*, vol. 17, no. 5, Sep. 2020, Art. no. 172988142093383.

[17] C. Jiang, L. Wan, Y. Sun, and Y. Li, "The application of PSO-AFSA method in parameter optimization for underactuated autonomous underwater vehicle control," *Math. Problems Eng.*, vol. 2017, pp. 1–14, Aug. 2017.

[18] J. Guerrero, J. Torres, V. Creuze, and A. Chemori, "Trajectory tracking for autonomous underwater vehicle: An adaptive approach," *Ocean Eng.*, vol. 172, pp. 511–522, Dec. 2019.

[19] D. Maalouf, A. Chemori, and V. Creuze, "Adaptive depth and pitch control of an underwater vehicle with real-time experiments," *Ocean Eng.*, vol. 98, pp. 66–77, Apr. 2015.

[20] S. M. Zanoli and G. Conte, "Remotely operated vehicle depth control," *Control Eng. Pract.*, vol. 11, no. 4, pp. 453–459, Apr. 2003.

[21] J. Ma, K. Liu, and C. Tan, "Finite-time robust containment control for autonomous surface vehicle with input saturation constraint," *Ocean Eng.*, vol. 252, May 2022, Art. no. 111111.

[22] D. Wang, C. Liu, D. Ding, S. Gao, and M. Chu, "Finite-time optimal tracking control using augmented error system method," *Appl. Math. Comput.*, vol. 424, Jul. 2022, Art. no. 127013.

[23] Z. Lv, Q. Zhao, S. Li, and Y. Wu, "Finite-time control design for a quadrotor transporting a slung load," *Control Eng. Pract.*, vol. 122, May 2022, Art. no. 105082.

[24] B. Chen, J. Hu, Y. Zhao, and B. K. Ghosh, "Finite-time velocity-free observer-based consensus tracking for heterogeneous uncertain AUVs via adaptive sliding mode control," *Ocean Eng.*, vol. 237, Oct. 2021, Art. no. 109565.

[25] G. Xia, Y. Zhang, W. Zhang, K. Zhang, and H. Yang, "Robust adaptive super-twisting sliding mode formation controller for homing of multi-underactuated AUV recovery system with uncertainties," *ISA Trans.*, Apr. 2022, doi: 10.1016/j.isatra.2022.04.010.

[26] G. Xia, Y. Zhang, W. Zhang, X. Chen, and H. Yang, "Dual closed-loop robust adaptive fast integral terminal sliding mode formation finite-time control for multi-underactuated AUV system in three dimensional space," *Ocean Eng.*, vol. 233, Aug. 2021, Art. no. 108903.

[27] Q. Wang, J. Cao, and H. Liu, "Adaptive fuzzy control of nonlinear systems with predefined time and accuracy," *IEEE Trans. Fuzzy Syst.*, early access, Apr. 25, 2022, doi: 10.1109/TFUZZ.2022.3169852.

[28] J. D. Sánchez-Torres, E. N. Sanchez, and A. G. Loukianov, "Predefined-time stability of dynamical systems with sliding modes," in *Proc. Amer. Control Conf. (ACC)*, 2015, pp. 5842–5846.

[29] N. Mazhar, F. M. Malik, A. Raza, and R. Khan, "Predefined-time control of nonlinear systems: A sigmoid function based sliding manifold design approach," *Alexandria Eng. J.*, vol. 61, no. 9, pp. 6831–6841, Sep. 2022.

[30] L. Lin, J. Zheng, P. Zhu, and D. Yang, "Predefined-time stability control method based on Lyapunov function," *J. Huazhong Univ. Sci. Technol., Natural Sci. Ed.*, pp. 1–6, Apr. 2022, doi: 10.13245/j.hust.228230.

[31] H. Sai, Z. Xu, S. He, and E. Zhang, "Predefined-time sliding mode control for rigid spacecraft," *Opt. Precis. Eng.*, vol. 29, no. 12, pp. 2891–2901, 2021.

[32] Y. Wang, Z. Wang, M. Chen, and L. Kong, "Predefined-time sliding mode formation control for multiple autonomous underwater vehicles with uncertainties," *Chaos, Solitons Fractals*, vol. 144, Mar. 2021, Art. no. 110680.

[33] T. I. Fossen, *Marine Control Systems: Guidance, Navigation and Control of Ships, Rigs and Underwater Vehicles*. Trondheim, Norway: Marine Cybernetics, 2002.

[34] M. Fu, T. Wang, and C. Wang, "Fixed-time trajectory tracking control of a full state constrained marine surface vehicle with model uncertainties and external disturbances," *Int. J. Control, Autom. Syst.*, vol. 17, no. 6, pp. 1331–1345, Jun. 2019.

[35] S. P. Bhat and D. S. Bernstein, "Finite-time stability of continuous autonomous systems," *SIAM J. Control Optim.*, vol. 38, no. 3, pp. 751–766, Jan. 2000.

[36] Z. Zuo, B. Tian, M. Defoort, and Z. Ding, "Fixed-time consensus tracking for multi-agent systems with high-order integrator dynamics," *IEEE Trans. Autom. Control*, vol. 63, no. 2, pp. 563–570, Feb. 2017.

[37] A. Polyakov, "Nonlinear feedback design for fixed-time stabilization of linear control systems," *IEEE Trans. Autom. Control*, vol. 57, no. 8, pp. 2106–2110, Aug. 2012.

[38] A. K. Pal, S. Kamal, S. K. Nagar, B. Bandyopadhyay, and L. J. A. Fridman, "Design of controllers with arbitrary convergence time," *Automatica*, vol. 112, Feb. 2020, Art. no. 108710.

[39] E. J. Rodriguez, J. D. S. Torres, and A. G. Loukianov, "Optimal predefined-time stabilization for a class of linear systems," *Ingeniería Electrónica Automática Y Comunicaciones*, vol. 38, no. 1, pp. 90–101, 2017.

[40] A. Weil, *Die Grundlehren der Mathematischen Wissenschaften*. Berlin, Germany: Springer-Verlag, 1974, pp. 106–115.

[41] A. P. Sergey Parsegov and P. Shcherbakov, "Fixed-time consensus algorithm for multi-agent systems with integrator dynamics," *IFAC Proc. Volumes*, vol. 46, no. 27, pp. 110–115, 2013.

[42] N. Ali, I. Tawiah, and W. Zhang, "Finite-time extended state observer based nonsingular fast terminal sliding mode control of autonomous underwater vehicles," *Ocean Eng.*, vol. 218, Dec. 2020, Art. no. 108179.

[43] J. Zheng, L. Song, L. Liu, W. Yu, Y. Wang, and C. Chen, "Fixed-time sliding mode tracking control for autonomous underwater vehicles," *Appl. Ocean Res.*, vol. 117, Dec. 2021, Art. no. 102928.

GUOYAN YU received the Ph.D. degree from the School of Mechanical & Automotive Engineering, South China University of Technology, Guangzhou, China, in 2001. She is currently a Professor with the School of Mechanical Engineering, Guangdong Ocean University, Zhanjiang, China. Her current research interests include intelligent optimization design and applications of artificial intelligence.

ZHUOCHENG LI received the B.E. degree from the School of Mechanical and Vehicle Engineering, Zhaoqing University, Zhaoqing, China, in 2020. He is currently pursuing the master's degree in mechanical engineering with Guangdong Ocean University. His research interests include adaptive control and motion control of remotely operated vehicles (ROVs).

HAITAO LIU (Member, IEEE) received the Ph.D. degree from the School of Mechanical & Automotive Engineering, South China University of Technology, Guangzhou, China, in 2012. He is currently a Professor with the School of Mechanical Engineering, Guangdong Ocean University, Zhanjiang, China. His current research interests include the theory and applications of nonlinear control and robotics.

QIHENG ZHU received the B.E. degree from the School of Mechanical and Power Engineering, Guangdong Ocean University, Zhanjiang, China, in 2020, where he is currently pursuing the master's degree in mechanical engineering. His research interests include intelligent product design and theory, nonlinear control, and fault-tolerant control theory.

• • •